

Biotransformation of Uranium Compounds in High Ionic Strength Brine by a Halophilic Bacterium under Denitrifying Conditions

A. J. FRANCIS,*† C. J. DODGE,†
J. B. GILLOW,† AND H. W. PAPENGUTH‡
Environmental Sciences Department, Brookhaven National Laboratory, Upton, New York 11973, and Chemical Processes Department, Sandia National Laboratories, Albuquerque, New Mexico 87185

We investigated the transformations of uranyl nitrate, uranyl citrate, uranyl ethylenediaminetetraacetate (U–EDTA), and uranyl carbonate by a denitrifying halophilic bacterium, *Halomonas* sp. (WIPP1A), isolated from the Waste Isolation Pilot Plant (WIPP) repository. The addition of uranyl nitrate, uranyl citrate, or uranyl EDTA to the brine or bacterial growth medium resulted in the precipitation of uranium. Extended X-ray absorption fine structure (EXAFS) analysis of the precipitates formed in the brine and in the growth medium were identified as uranyl hydroxide [UO₂(OH)₂] and uranyl hydroxophosphato species [K(UO₂)₅(PO₄)₃(OH)₂·nH₂O], respectively. Dissolution of the uranium precipitate was concomitant with the growth of the bacteria under anaerobic conditions. The UV–vis spectra of the culture medium during growth showed that a uranyl dicarbonate complex [UO₂(CO₃)₂]²⁻ was formed due to CO₂ production from the metabolism of the carbon source succinate. The bacterium completely metabolized the citrate released from the uranyl citrate complex but not the EDTA released from the U–EDTA complex. Adding uranyl carbonate to the growth medium caused no changes in the uranium speciation due to bacterial growth. Uranyl carbonate was not biosorbed by the growing culture nor by washed resting cells suspended in 20% NaCl brine (3.4 M) because the complex was either neutral or anionic. Our results demonstrate that bacterial activity can enhance the dissolution of uranium phosphate by forming uranyl carbonate species.

Introduction

The actinides (Th, U, Np, Pu, Am) in transuranic (TRU) waste are present in various forms, i.e., ionic, inorganic complex, organic complex, coprecipitates, and minerals. In addition, TRU waste contains contaminated protective clothing, rags, paper, plastics, and nitrate. Currently, TRU waste is disposed of in deep geological salt formations at the Waste Isolation Pilot Plant (WIPP), Carlsbad, NM. Although much is known of the physical, chemical, geochemical, hydrological, and environmental factors that affect the long-term stability of the actinides and the waste forms, little is known of the

microbial effects (1). In particular, we have limited knowledge of the mechanisms of biotransformation of various chemical forms of actinides in TRU waste in a high ionic strength hypersaline environment such as the WIPP repository.

Under appropriate conditions, microorganisms can affect the mobilization or immobilization of actinides in the waste repository by direct enzymatic or indirect nonenzymatic actions (2). Microbes also can affect the transport of actinides by forming biocolloids (3–5). Fundamental information on the mechanisms of microbial transformations of actinides under various environmental conditions is useful in predicting the fate and long-term transport of actinides in waste repositories as well as developing strategies for managing waste. At the WIPP site, natural populations of halophilic bacteria range from 10⁴ to 10⁷ cells mL⁻¹ (6), and the numbers are likely to increase due to biodegradation of the organic constituents of the TRU waste. An increase in microbial activity can affect the solubility, bioavailability, and mobility of actinides in the repository.

In this paper, we describe the biotransformation of several uranium compounds (i.e., uranyl nitrate, uranyl citrate, U–EDTA, and uranyl carbonate) added to the bacterial growth medium under denitrifying conditions by a halophilic bacterium isolated from the WIPP repository.

Materials and Methods

Bacterial Culture. *Halomonas* sp. (WIPP1A) was isolated from a sediment slurry sample from the WIPP site (6). The bacterium grows rapidly aerobically or anaerobically using nitrate as an electron acceptor, reduces nitrate to N₂, but does not reduce iron or uranium. The bacterium was grown in a medium containing 5.0 g of sodium succinate, 1.0 g of KNO₃, 0.25 g of K₂HPO₄, 0.5 g of yeast extract, 200 g of WIPP salt (halite), and 1000 mL of deionized water at pH 6.5. The operational pH (uncorrected for ionic strength) was measured with an AgCl combination electrode using a Beckman φ-11 pH meter. This medium simulates the Castile brine formation below the repository's horizon (3). The medium was pre-reduced by purging with filtered ultrahigh-purity (UHP) N₂ gas and then was filter-sterilized through 0.45-μm Nalgene sterile filters. A total of 95 mL of the medium was dispensed into 160-mL acid-washed sterile (autoclaved) glass serum bottles in an anaerobic nitrogen-filled glovebox. The bottles were fitted with sterile butyl rubber stoppers and sealed with aluminum crimp seals. All manipulations were carried out in a glovebox in a N₂ atmosphere. The medium was inoculated with 1 mL of an early log-phase (24-h-old) culture of *Halomonas* sp. and incubated under static conditions in the dark at 30 ± 2 °C. Aliquots were withdrawn periodically from a well-mixed sample, and the total number of cells was enumerated by direct microscopy using the DAPI staining technique (7) and optical density measured at 600 nm using an HP8453A scanning UV–vis spectrophotometer.

Uranyl Nitrate. A stock solution of uranyl nitrate (355 mM) was prepared by dissolving UO₂(NO₃)₂·6H₂O (Analar, BDH Chemicals Ltd., Poole, England) in deionized water.

Uranium–Organic Complexes. An equimolar 1:1 U–citric acid complex or 1:1 U–EDTA complex (50 mM) was prepared by slowly combining an appropriate amount of anhydrous citric acid or Na₂EDTA·2H₂O (Sigma, St. Louis, MO) with a uranyl nitrate stock solution while constantly mixing it. The pH of the solution was adjusted to 6.5.

Uranyl Carbonate. A 1:10 uranyl carbonate complex (50 mM) was prepared by combining Na₂CO₃ stock solution (prepared in boiled and N₂-purged deionized water) with a uranyl nitrate stock solution in a nitrogen-flushed beaker

* Corresponding author e-mail: francis1@bnl.gov; phone: (631)-344-4534; fax: (631)344-7303.

† Brookhaven National Laboratory.

‡ Sandia National Laboratories.

with constant stirring. The pH was adjusted to 7.5 by adding 6 M HCl. Care was taken to minimize the exposure of the solution to air. The presence of uranyl carbonate complex was confirmed by measuring the absorption spectra between 350 and 550 nm and comparing it with the known spectra using a HP8453A scanning UV-vis spectrophotometer (8, 9). All uranium complexes were stored in the dark to prevent photodecomposition (10).

Biotransformation of Uranium. A total of 100 mL of 0.45 μm (Nalgene) filter-sterilized and N_2 -purged bacterial growth medium was added to sterile 160-mL glass serum bottles inside a N_2 -filled glovebox. Stock solutions of uranyl nitrate, uranyl citrate, U-EDTA, or uranyl carbonate were purged with N_2 for 15 min, filter-sterilized by using a 0.45- μm filter, and added to the growth medium so that the final concentration of uranium was 1.05×10^{-3} M except for uranyl citrate, which was 0.52×10^{-3} M. The nitrate concentration in the growth medium was adjusted to give the same final concentration in all treatments. Triplicate samples of each medium were inoculated with 2.5 mL of 24-h-old culture of *Halomonas* sp. and incubated at 30 ± 2 °C under static conditions. Uninoculated samples in duplicate were included for each treatment as abiotic controls.

At periodic intervals before sampling, the bottles were thoroughly shaken, and 9 mL of the medium was removed with a sterile syringe. A total of 1 mL was preserved with 0.05 mL of formalin (5% v/v) for cell counts and 3 mL for measuring pH and turbidity. The remaining sample (5 mL) was filtered through a 0.22- μm disposable Whatman Puradisc syringe filter unit, the UV-vis spectra was recorded, and the sample was then acidified with 0.1 mL of concentrated HCl for citric acid, succinic acid, and uranium analyses. The uranium association with bacterial cells at the stationary growth phase of the culture was determined after recovering the cells by centrifugation, washing them twice with 20% NaCl solution, and digesting with concentrated HNO_3 .

Biosorption of Uranyl Carbonate by Resting Cells. To determine whether the uranyl carbonate formed during the growth was biosorbed by the bacterial cells, the culture was grown in growth medium containing succinate without uranium under anaerobic conditions as described before. The cells were harvested after 72 h by centrifugation at 5000g for 15 min. The cell pellet was washed twice with 20% NaCl solution at pH 5, which earlier had been purged with N_2 and filter-sterilized by passing through a 0.45- μm filter. The cells were resuspended in 20% NaCl solution to an optical density of 0.8 ($\sim 10^8$ cells mL^{-1}), and the pH was adjusted to 9.0 with NaOH. The cell suspension (35 mL) was placed in a Mettler DL-53 automated titrator. The titration vessel was continuously purged with N_2 to exclude air, and the cells were equilibrated at pH 9 using a Mettler DG111 electrode for 90 min. Uranyl carbonate complex was added to give a final uranium concentration of 0.125 mM. The sample was adjusted to pH 9 and incubated for 1 h. To determine uranium uptake by the cells, an aliquot of the sample was removed and filtered through a 0.22- μm Millex filter (Millipore, MA), and the filtrate was acidified with 5% v/v HNO_3 and analyzed for uranium.

Effect of Bacterial Growth Medium Components on Uranium Solubility. Addition of uranyl nitrate, uranyl citrate, or U-EDTA complex to the bacterial growth medium resulted in the precipitation of uranium. To determine which of the components of the growth medium was involved in precipitating U, we added uranyl nitrate, uranyl citrate or U-EDTA to 20% NaCl solution containing the following components: (i) no addition, (ii) sodium succinate (5 g/L), (iii) K_2HPO_4 (0.25 g/L), (iv) yeast extract (0.5 g/L), and (v) complete growth medium containing all of the above. The pH of the medium was adjusted to 6.5. After 6 h, the medium was centrifuged at 7000g to separate the precipitate. The

precipitate was dissolved in a solution of sodium bicarbonate (0.07 M) and analyzed for phosphorus, potassium, and uranium by ICP-AES. The supernatant was analyzed for succinic acid, citric acid, or EDTA by high-pressure liquid chromatography (HPLC) and for uranium.

Characterization of the Uranium Precipitate. X-ray diffraction (XRD) analysis of the precipitate obtained from addition of uranium to the growth medium was performed using a Philips XRG-3100 analyzer with a $\text{Cu K}\alpha$ X-ray source. The uranium precipitates recovered from adding uranium nitrate to the brine solution and the growth medium were analyzed by extended X-ray absorption fine structure (EXAFS). The precipitate was placed in a heat-sealed polyethylene bag (0.2%) and analyzed on the X-18B beamline at the National Synchrotron Light Source (NSLS) with a Si(111) channel-cut crystal at the uranium L_{III} absorption edge (17.166 keV) using a fluorescence detector with an Ar-filled ion chamber (11). The monochromator was detuned by 30% to attenuate the beam's harmonics. Multiple scans (up to 12) were collected, the individual spectra were deglitched, and the scans were averaged.

Uranyl hydrogen phosphate was synthesized by slowly adding 0.42 M uranyl nitrate solution to 0.84 M phosphoric acid (12). The resulting precipitate was washed in acetone and dried at 105 °C. X-ray diffraction analysis confirmed that $\text{UO}_2\text{HPO}_4 \cdot 2\text{H}_2\text{O}$ was formed (JCPDS 13-61). A multistep data analysis of the k^3 -weighted EXAFS spectra in the k range of 3.6–12.5 \AA^{-1} included Fourier transformation of the normalized spectra. The theoretical EXAFS modeling code FEFF7 was used to calculate the backscattering phase and amplitude information for individual neighboring atoms (13). Fitting parameters for the sample then were obtained by comparison with the uranyl hydrogen phosphate standard.

Organic Acid Analysis. Citric and succinic acids were analyzed by HPLC after 10-fold dilution, followed by filtration through a 0.22- μm filter. The organic acids were separated on a Bio-Rad Aminex HPX-87H ion exclusion column and analyzed using a Shimadzu SPD-10A UV-vis detector at 210 nm. For EDTA analysis, the samples were pretreated with 0.07 g/L ferric ion, separated on a Nucleosil C-18 (250 mm \times 4.6 mm) reversed-phase ion-pair column maintained at 50 °C, and analyzed using a UV-vis detector at 254 nm. The mobile phase consisted of 0.03 M acetic acid and counterion tetrabutylammonium hydroxide (14).

Uranium Analysis. All samples were filtered through a 0.22- μm Millex filter (Millipore, MA) and analyzed for uranium using a Varian Liberty 150 ICP-AES.

Carbon Dioxide Production. The total amount of CO_2 produced by the bacteria incubated for 120 h was determined in separate samples after adding 1 mL of concentrated perchloric acid. Carbon dioxide in the headspace was analyzed by a Varian 3400 gas chromatograph fitted with a Porapak QS (Alltech, IL) column (2 m \times 3.2 mm) and a thermal conductivity detector with He as the carrier gas. The column temperature was maintained at 100 °C, the detector at 250 °C, and the filament current at 225 mA. Gas calibration standards (Scotty II) were obtained from Scott Specialty Gases, New Jersey.

Results

Effect of Growth Medium Components on Uranium Solubility. The addition of uranyl nitrate or U-EDTA to (i) brine, (ii) brine plus succinate, (iii) brine plus phosphate, (iv) brine plus yeast extract, or (v) growth medium containing all the ingredients at pH 6.0 precipitated uranium. In contrast, adding uranyl citrate to (i) brine, (ii) brine plus succinate, or (iii) brine plus yeast extract did not precipitate uranium. However, uranium precipitated out when uranyl citrate was added to brine containing phosphate or growth medium.

TABLE 1. Chemical Characterization of Uranium Precipitate in Growth Medium

element ^a	μmol^b
uranium	22.5 ± 0.3
phosphorus	13.6 ± 0.0
potassium	4.2 ± 1.0

^a 40 mg of sample dissolved in 0.07 M sodium bicarbonate. ^b ± 1 SEM.

Characterization of the Uranium Precipitate. *Chemical Analysis.* Table 1 lists the chemical constituents of the precipitate obtained from addition of uranium to the growth medium. The 40-mg sample contained $22.5 \mu\text{mol}$ of U, $13.6 \mu\text{mol}$ of P, and $4.2 \mu\text{mol}$ of potassium; no succinic acid, citric acid, or EDTA were detected.

XRD analysis of the precipitate showed that NaCl was the predominant crystalline phase, and uranium was present in an amorphous form.

Figure 1A shows the EXAFS analysis of the precipitate resulting from adding uranyl nitrate to brine solution. A three-shell fit of the k^3 -weighted spectrum for the uranyl hydroxide standard duplicates the oscillations fairly well, except for the feature at 10.5 \AA^{-1} . Uranyl hydroxide has four hydroxide groups surrounding the central uranium, two of which act asolation bridges to another uranium at $3.9\text{--}4.2 \text{ \AA}$. The precipitate resulting from the addition of uranyl nitrate to brine shows similar spectra, but the feature at 10.5 \AA is more pronounced. Addition of a U shell at 4.2 \AA duplicates the feature but does not improve the overall fit of the data set and was not included in the fits.

Fourier transformed spectra for the brine precipitate is shown in Figure 1B. The peaks represent coordination shells at radial distances from the central uranium atom. A variation in the amplitude of the shells is due to differences in coordination number or atomic distances in the uranium inner sphere (15). There are some differences in the atomic environment surrounding the precipitate as compared to uranyl hydroxide. Table 2 shows the presence of 1.8 axial oxygens at 1.80 \AA from the uranium in the hydroxide, while the precipitate shows 2.3 oxygens. There is a split in the equatorial shell of the hydroxide in both samples with 2.3 oxygens at 2.25 \AA and 1.3 oxygens at 2.49 \AA for uranyl hydroxide and with 3.2 oxygens at 2.24 \AA and 1.5 oxygens at 2.50 \AA for the precipitate. The additional oxygen found in the first equatorial shell of the precipitate indicates a change in bonding in the equatorial oxygens closest to the uranium and is probably due to the high ionic strength of the brine that may influence hydroxide formation. No chloride was detected in the precipitate.

Analysis of the EXAFS spectral data for the precipitate resulting from the addition of uranyl citrate complex to the growth medium was obtained by comparison with the uranyl hydrogen phosphate standard. The atomic parameters for the standard and this precipitate were obtained by fitting k^3 -weighted EXAFS spectra; the results are presented in Figure 2A and Table 3. A three-shell fit showed good agreement with both the standard and the sample. The feature at 9.0 \AA^{-1} is typical for a U-P interaction.

Figure 2B depicts the Fourier transformed spectra for uranyl hydrogen phosphate and the uranium precipitate over the k range $3.6\text{--}12.5 \text{ \AA}^{-1}$. The peak at 2.4 \AA in the fitted spectra may reflect multiple scattering processes or a side lobe resulting from truncation effects. Shells further from uranium also are indicated, but interpretation is difficult due to multiple scattering effects as well as structural disorder in the samples. Uranyl hydrogen phosphate is composed of a uranyl moiety (2 axial O's at 1.75 \AA) surrounded by four equatorial oxygens at 2.30 \AA , which in turn occupy the corners

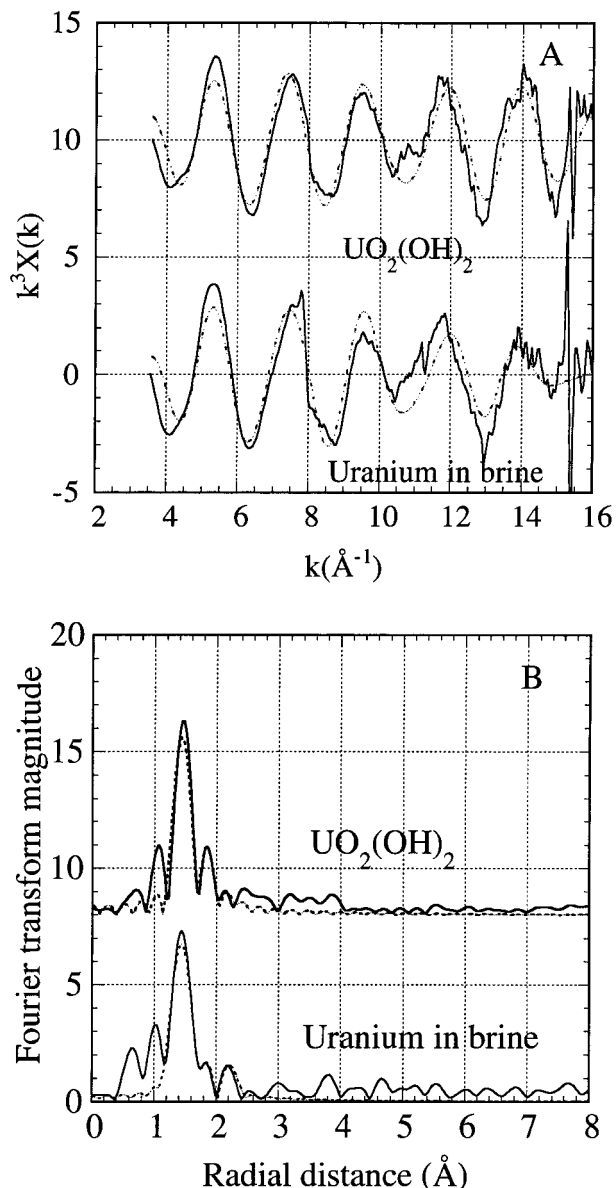


FIGURE 1. Raw $U_{L_{III}}$ k^3 -weighted EXAFS data (A) and corresponding Fourier transforms (B) ($k = 3.6\text{--}16.1 \text{ \AA}^{-1}$) for uranyl hydroxide and the precipitate resulting from adding uranyl nitrate to brine. Experimental data (—); theoretical fit (---).

TABLE 2. Coordination Number (N), Interatomic Distance (R), Disorder Parameter (σ^2), and Goodness of Fit Parameter (F) for Precipitate Resulting from Adding Uranyl Nitrate to Brine

sample	atom	N	$R(\text{Å})$	σ^2	F
$UO_2(OH)_2$	U-O _{ax}	1.8	1.80	0.0010	0.06
	U-O _{eq1}	2.3	2.25	0.0032	0.01
	U-O _{eq2}	1.3	2.49	0.0030	0.01
uranium in brine	U-O _{ax}	2.3	1.80	0.0032	0.02
	U-O _{eq1}	3.2	2.24	0.0091	0.02
	U-O _{eq2}	1.5	2.50	0.0020	0.01

of a phosphate tetrahedron (Table 3). The four phosphorus atoms are separated from the uranium by 3.54 \AA . The precipitate is similar in structure to the phosphate standard and has 2 axial oxygens at 1.80 \AA , 4 equatorial oxygens at 2.30 \AA , and 4 phosphorus atoms at 3.59 \AA from the uranium. The Debye-Waller values (σ^2) derived from room temperature data are typical for the coordination numbers and static disorder of the atoms (16). The EXAFS spectra all were similar

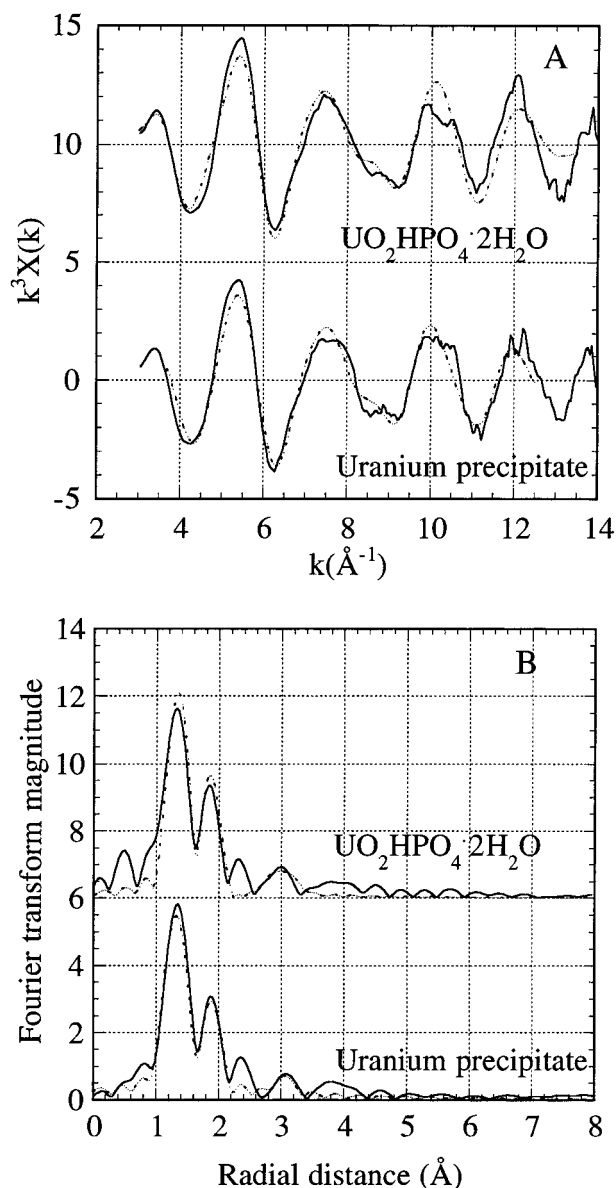


FIGURE 2. Raw U_{LIII} k^3 -weighted EXAFS data (A) and corresponding Fourier transforms (B) ($k = 3.6\text{--}12.5 \text{\AA}^{-1}$) for uranyl hydrogen phosphate and the precipitate resulting from addition of uranyl citrate to brine. Experimental data (—); theoretical fit (---).

TABLE 3. Coordination Number (N), Interatomic Distance (R), Disorder Parameter (σ^2), and Goodness of Fit Parameter (F) for Precipitate Resulting from Adding Uranyl Citrate to Growth Medium

sample	atom	N	$R(\text{\AA})$	σ^2	F
$\text{UO}_2\text{HPO}_4 \cdot 2\text{H}_2\text{O}$	U—O _{ax}	2.0	1.75	0.0034	0.12
	U—O _{eq}	4.0	2.30	0.0058	0.01
	U,P	4.0	3.54	0.0169	0.01
uranium precipitate	U—O _{ax}	2.0	1.80	0.0041	0.02
	U—O _{eq}	4.0	2.30	0.0037	0.01
	U,P	4.0	3.59	0.0124	0.01

for precipitates formed from the addition of uranium as uranyl nitrate, uranyl citrate, and U-EDTA to the growth medium.

Growth of Bacteria. Figure 3 shows plots of the growth of the bacteria under anaerobic conditions in a 20% NaCl growth medium containing succinate as the sole carbon source and nitrate as the electron acceptor. Maximum growth

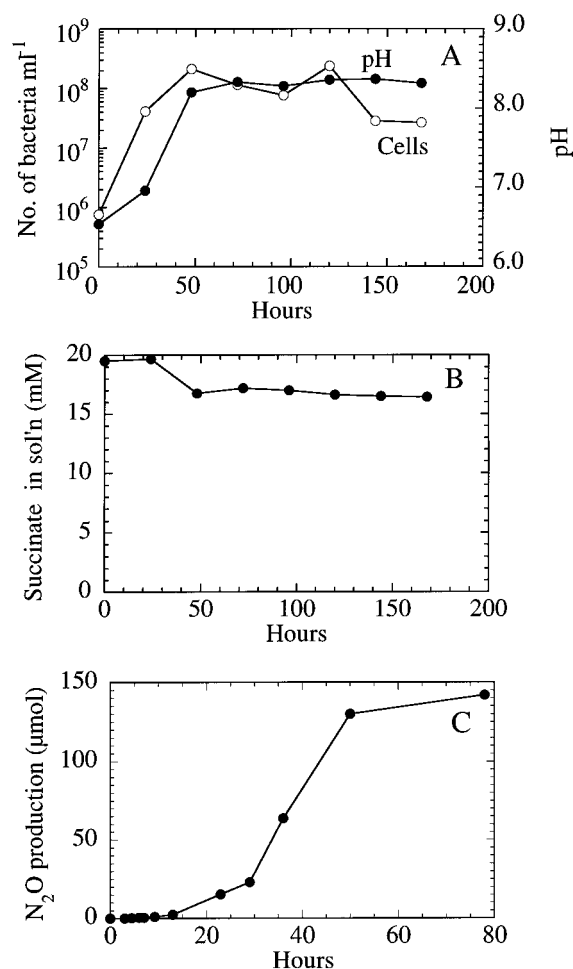


FIGURE 3. Growth of *Halomonas* sp. in brine medium. (A) Growth of bacteria and changes in pH of the medium; (B) metabolism of the carbon source succinic acid; and (C) production of N_2O by the culture grown anaerobically in the presence of nitrate as electron acceptor.

was attained in about 50 h with cell numbers increasing from 7.6×10^5 to 2.4×10^8 cells mL^{-1} (Figure 3A). The pH of the medium increased from 6.5 to 8.3 due to the metabolism of succinic acid, which decreased from 19.5 ± 0.1 to 16.4 ± 0.3 mM (Figure 3B). Nitrate was used both as a nitrogen source and as an electron acceptor, and the maximum denitrification rate was $5.1 \mu\text{mol}$ of N_2O h^{-1} (Figure 3C).

Uranyl Nitrate. The growth of the bacteria in the presence of 1.05 mM uranyl nitrate (Figure 4) was similar to that of the medium without uranium. The number of cells increased from 3.7×10^6 cells mL^{-1} to a maximum of 5.3×10^8 cells mL^{-1} within 50 h (Figure 4A). The pH of the medium increased from 6.8 to 8.3, and the concentration of succinic acid decreased from 18.7 to 16.8 mM. Adding uranyl nitrate to the growth medium immediately precipitated uranium (Figure 4B). Uranium dissolved concomitant with an increase in bacterial growth and reached a final concentration of 1.03 ± 0.01 mM. A change in the UV-vis absorption spectra of the filtered culture showed a change in its absorption characteristics that coincided with the increase in uranium concentration in solution (Figure 4C). The appearance of peaks at 434, 448, and 464 nm is characteristic of the uranyl dicarbonate species (8) and is due to CO_2 production by the bacterial activity.

Uranyl Citrate. Figure 5 depicts the growth of the bacteria in the presence of 0.52 mM uranyl citrate. As their number increased from 5.3×10^6 to 1.0×10^8 , the pH increased from

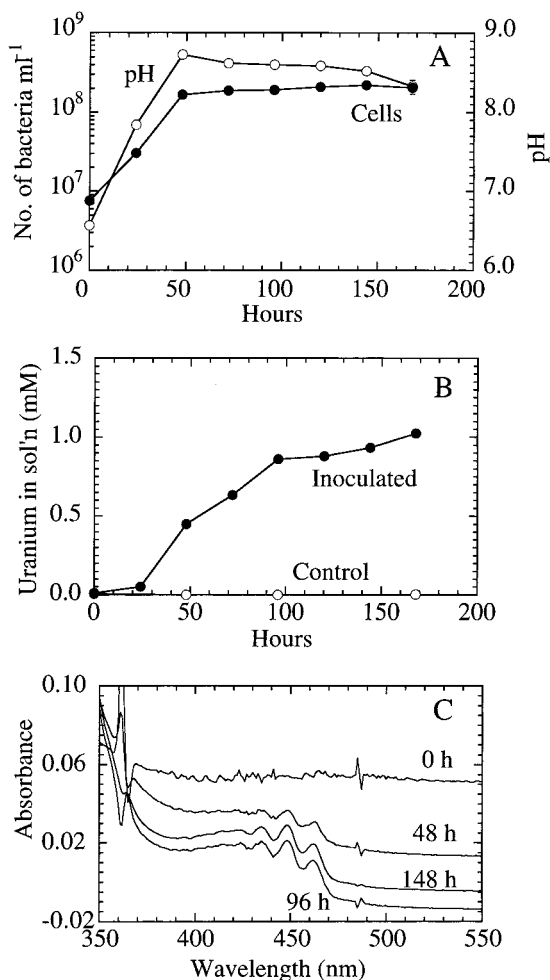


FIGURE 4. Growth of *Halomonas* sp. and biotransformation of uranium added as uranyl nitrate. (A) Growth of bacteria and changes in pH of the medium; (B) dissolution of uranium (1.05 mM uranyl nitrate was added to the growth medium and resulted in the precipitation of U); and (C) UV-vis spectra of the culture medium showing the formation of uranyl carbonate as a function of growth.

6.3 to 7.7. The addition of uranyl citrate to the growth medium caused the dissociation of the complex with the precipitation of uranium (Figure 5B). The citric acid released from the complex was completely metabolized by the bacteria at the rate of 1.2 mmol h⁻¹. The concentration of succinic acid decreased from 18.9 to 16.6 mM. The UV-vis spectra of the filtered culture solution during bacterial growth showed the appearance of uranyl dicarbonate species concurrent with uranium dissolution (Figure 5C).

U-EDTA. Figure 6 shows the growth of the bacterium in medium containing 1.05 mM U-EDTA. Cell numbers increased slowly from 2.1×10^6 to 1.6×10^8 cells mL⁻¹, and the pH increased to 7.8 from 6.7 (Figure 6A). Succinic acid concentration decreased from 17.1 to 15.6 mM. Addition of the U-EDTA complex to the growth medium completely precipitated uranium, with a 15% decrease in EDTA concentration in solution (Figure 6B). About 97% of the added uranium was solubilized with increased bacterial activity. The UV-vis spectra showed the appearance of uranium in solution as uranyl dicarbonate species (Figure 6C). The EDTA was not metabolized by the bacteria and remained at the concentration initially added to the medium.

Uranyl Carbonate. Figure 7 shows the growth of the bacteria in the presence of 1.05 mM uranyl carbonate complex. The number of cells increased from 2.0×10^6 to 1.9×10^8 , and the pH increased slightly from 7.5 to 7.9 (Figure

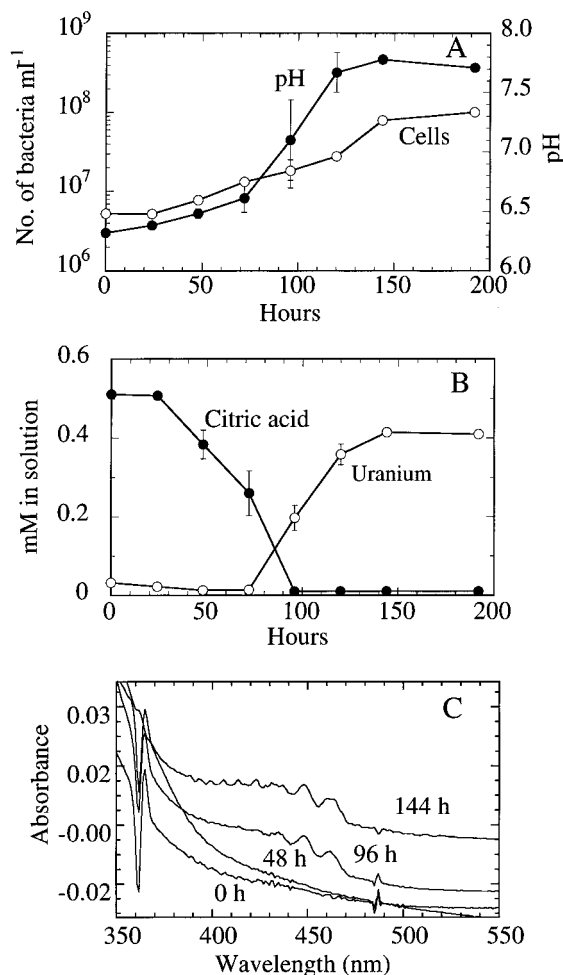


FIGURE 5. Growth of *Halomonas* sp. and biotransformation of uranium added as 1:1 U-citric acid complex. (A) Growth of bacteria and changes in pH of the medium; (B) dissolution of uranium (0.52 mM uranyl citrate was added to the medium and resulted in the precipitation of U); and (C) UV-vis spectra of the culture medium showing the formation of uranyl carbonate as a function of growth.

7A). The addition of uranyl carbonate to the growth medium initially caused a 15% decrease in uranium concentration from 1.05 to 0.89 ± 0.01 mM (Figure 7B). However, uranium was resolubilized as bacterial growth progressed and reached a final concentration of 1.1 ± 0.0 mM at 100 h. The UV-vis spectra of the filtered culture medium showed that the uranium was present as uranyl carbonate species during the experiment (Figure 7C). Uranium in the uninoculated control sample steadily decreased from 0.93 ± 0.02 to 0.69 ± 0.00 mM. EXAFS analysis of the uranium in solution and the precipitate formed in the uninoculated control and inoculated medium confirmed the presence of uranyl carbonate. The spectral characteristics are similar to those observed by others (9, 17).

Carbon Dioxide Production by the Culture. The total amount of CO₂ produced by the culture in the presence of succinate ($32.0 \mu\text{mol mL}^{-1}$), uranyl nitrate ($29.0 \mu\text{mol mL}^{-1}$), and uranyl citrate ($30.7 \mu\text{mol mL}^{-1}$) was similar except in the uranyl carbonate medium ($60.9 \mu\text{mol mL}^{-1}$), which showed a 2-fold increase due to the addition of carbonate.

Biosorption of Uranyl Carbonate by Resting Cells. Resting cells at pH 9 did not biosorb the inorganic uranyl carbonate complex because the most probable forms in solution are neutral (UO₂CO₃) or negatively charged species UO₂(CO₃)₂²⁻. Also, in the growth experiments, solubilized uranium was not biosorbed.

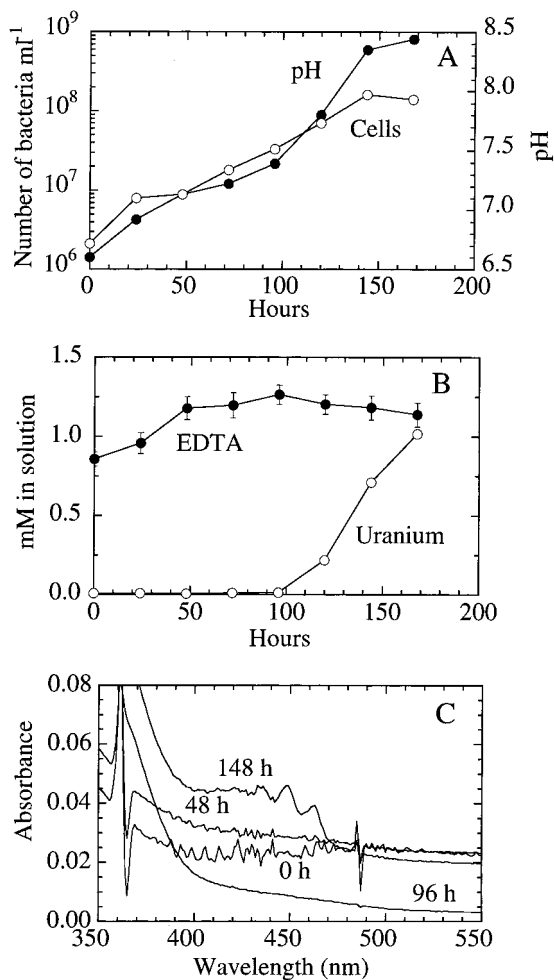
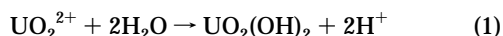


FIGURE 6. Growth of *Halomonas* sp. and biotransformation of uranium added as 1:1 U-EDTA complex. (A) Growth of bacteria and changes in pH of the medium; (B) dissolution of uranium (1.05 mM U-EDTA complex was added to the medium and resulted in the precipitation of U); and (C) UV-vis spectra of the culture medium showing the formation of uranyl carbonate as a function of growth.

Discussion

Although much is known of the behavior of uranyl compounds in very acidic and low ionic strength solutions, little is known of the stability, the solubility, and the chemical speciation of the various inorganic and organic complexes of uranium in high ionic strength solutions at physiological pH (pH = 6–8). In aqueous solution at near-neutral pH, uranium (added as uranyl nitrate) precipitates as uranyl hydroxide. Above pH 3, uranium is present as mono- and dihydroxy species at low concentration ($<10^{-4}$ M) and as polymeric species at higher concentration (17). The complexation of the uranyl ion by EDTA was investigated in solutions containing 0.3–5 M NaCl in the pCH range of 2–4.5; $\text{UO}_2\text{EDTA}^{2-}$ and $\text{UO}_2\text{HEDTA}^-$ complexes were identified (18). At pCH above 4.0, uranium was significantly hydrolyzed. There was a slight dependence upon ionic strength between 1 and 5 M NaCl. The 1:1 U-EDTA complex ($\log K$ 7.4) in aqueous solution above pH 6.5 dissociates due to formation of hydroxy species and uranium precipitates from solution (19). We confirmed the formation of uranyl hydroxide species when uranyl nitrate or U-EDTA was added to 20% brine above pH 5 (eq 1).



The formation of 1:1 and 1:2 uranyl citrate complexes in 5 M brine at pCH 6.0 and 7.0 was observed, and the stability

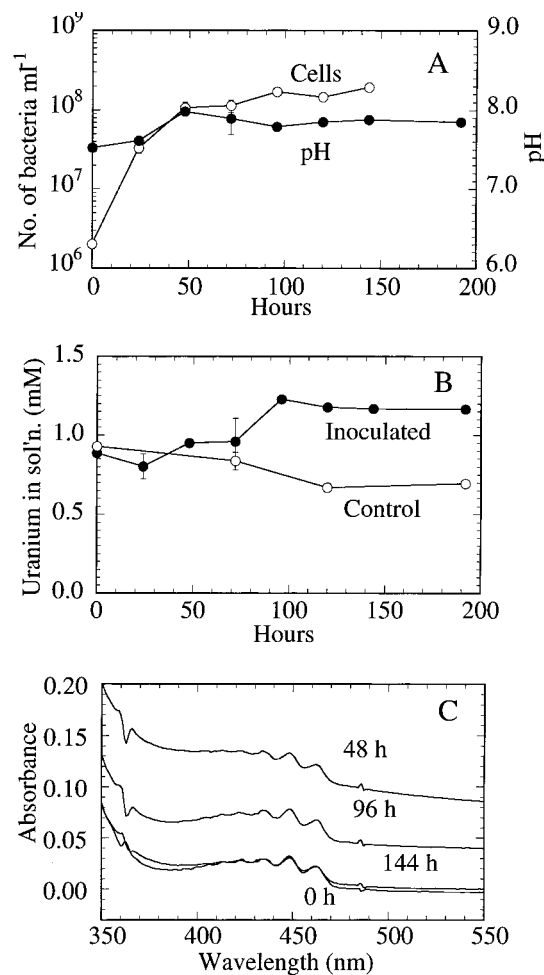
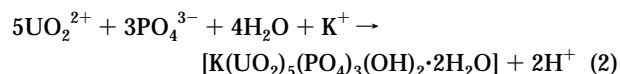


FIGURE 7. Growth of *Halomonas* sp. in the presence of uranyl carbonate complex. (A) Growth of bacteria and changes in pH of the medium; (B) uranium in the inoculated and uninoculated control medium; and (C) UV-vis spectra of the culture medium showing the presence of uranyl carbonate as a function of growth.

constants ($\log k$) were calculated to be 6.04 and 10.98, respectively (20). These values are orders of magnitude greater than those of uranyl acetate, uranyl lactate, U-EDTA, and uranyl ascorbate complexes. These studies also indicated that the concentration of citrate needed to compete with hydrolysis reactions at pCH 6.0 to obtain 10% hydrolysis in brine was the lowest of all organics tested, thereby contributing significantly to the dissolution of uranium. Citric acid has been shown to form a binuclear complex with uranium that may prevent its hydrolysis (21).

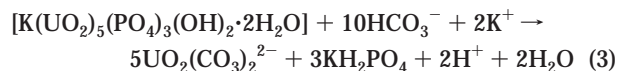
Adding uranyl nitrate, uranyl citrate, or U-EDTA to the bacterial growth medium at near-neutral pH (6.5) completely precipitated uranium from solution. Precipitation of uranium after the addition of uranyl citrate complex to the growth medium components was observed only in the presence of phosphate. The solubility of uranyl phosphate is 2×10^{-13} M. Elemental analysis and EXAFS confirm that uranium is predominantly associated with the phosphate ligand as $\text{K}(\text{UO}_2)_3(\text{PO}_4)_3$ and most likely consists of uranyl orthophosphate ($\text{UO}_2)_3(\text{PO}_4)_2$ units due to the interaction with phosphate present in the growth medium. The formation of the precipitate is presented in eq 2.



The addition of uranyl nitrate to a solution of sodium phosphate resulted in the formation of $(\text{UO}_2)_3(\text{PO}_4)_2$ (22).

Thompson et al. (16) demonstrated that the uranyl ion is surrounded by phosphate tetrahedra. This also was observed for the uranyl hydroxophosphato complexes where $[(\text{UO}_2)_3(\text{OH})_2]^{2n-}$ chains are linked by phosphate tetrahedra to give infinite layers of $[(\text{UO}_2)_3(\text{PO}_4)_2(\text{OH})_2]$ (23). EXAFS analysis of uranyl nitrate in acidic solutions containing 1–14 M HCl has shown that increased chloride ion leads to inner-sphere chloride complexation, decrease in hydration numbers, and expansion of the uranium–oxygen bond lengths (15). However, in our experiments uranyl phosphate was identified but the presence of an inner-sphere chloride bound to uranyl ion was not evident.

The uranium precipitate was solubilized by adding bicarbonate to the precipitate, or alternatively by the production of CO_2 from the bacterial metabolism of the carbon source succinate, with the formation of uranyl dicarbonate (eq 3).



The carbonate ion is one of the most environmentally important inorganic complexing agents of uranium. The speciation and the solubility of uranyl carbonate in aqueous solutions have been extensively studied (17, 24). Uranyl carbonate can be present as mono-, di-, and tricarbonato species depending on the pH as well as carbonate concentration in solution. The monomeric and dimeric uranyl carbonate species predominate above pH 5; at uranyl concentrations above 1 mM, the trimeric species is favored. Spectroscopic analysis of the carbonate species indicate the presence of uranium in the dicarbonate form $[\text{UO}_2(\text{CO}_3)_2]^{2-}$ (log K 16.2). We have demonstrated that an increase in microbial activity can enhance uranium dissolution due to formation of the soluble uranyl carbonate species. Additional studies are needed to determine the extent of microbial dissolution of uranium associated with various phosphate minerals.

Acknowledgments

This work was conducted under the auspices of the U.S. Department of Energy Contract DE-AC02-76CH00016 through a subcontract from Sandia National Laboratories, Albuquerque, NM.

Literature Cited

- (1) National Research Council. *The Waste Isolation Pilot Plant. A potential solution for the disposal of transuranic waste*; National Academy Press: Washington, DC, 1996.

- (2) Francis, A. J. *J. Alloys Compd.* **1998**, 271–273, 78–84.
- (3) *Mobile Colloid Actinide Source Term*, Appendix SOTERM 6, Title 40 CFR Part 191, Compliance Certification Application for the Waste Isolation Pilot Plant; DOE/CAO-1996-2184; U.S. Department of Energy, Waste Isolation Pilot Plant, Carlsbad Area Office: Carlsbad, NM, 1996; <http://reserve.wipp.carlsbad.nm.us> (accessed Feb 2000).
- (4) Francis, A. J.; Gillow, J. B.; Dodge, C. J.; Dunn, M.; Mantione, K.; Strietelmeier, B. A.; Pansoy-Hjelvik, M. E.; Papenguth, H. W. *Radiochim. Acta* **1998**, 84, 347–354.
- (5) Gillow, J. B.; Dunn, M.; Francis, A. J.; Lucero, D. A.; Papenguth, H. W. *Radiochim. Acta*, in press.
- (6) Francis, A. J.; Gillow, J. B.; Giles, M. R. *Microbial Gas Generation Under Expected Waste Isolation Pilot Plant Repository Conditions*; SAND96-2582; Sandia National Laboratories: Albuquerque, NM, 1997.
- (7) Kepner, R. L.; Pratt, J. R. *Microbiol. Rev.* **1994**, 58, 603–615.
- (8) McClaine, L. A.; Bullwinkel, E. P.; Huggins, J. C. *The carbonate chemistry of uranium: Theory and applications*; Proceedings of the International Conference on the Peaceful Uses of Atomic Energy, Geneva: United Nations: New York, 1956; Vol. 8, pp 26–37.
- (9) Meinrath, G. J. *Radioanal. Nucl. Chem.* **1997**, 224, 119–126.
- (10) Dodge, C. J.; Francis, A. J. *Environ. Sci. Technol.* **1994**, 28, 1300–1306.
- (11) Sayers, D. E.; Stern, E. A.; Lytle, F. *Phys. Rev. Lett.* **1971**, 27, 1204–1207.
- (12) Pekarek, V.; Benesova, M. J. *Inorg. Nucl. Chem.* **1964**, 26, 1743–1751.
- (13) Ankudinov, A. Ph.D. Thesis, University of Washington, 1996.
- (14) Bergers, P. J. M.; de Groot, A. C. *Water Res.* **1994**, 28, 639–642.
- (15) Allen, P. G.; Bucher, J. J.; Shuh, D. K.; Edelstein, N. M.; Reich, T. *Inorg. Chem.* **1997**, 36, 4676–4683.
- (16) Thompson, H.; Brown, G. E.; Parks, G. A. *Am. Mineral.* **1997**, 82, 483–496.
- (17) Clark, D. L.; Hobart, D. E.; Neu, M. P. *Chem. Rev.* **1995**, 95, 25–48.
- (18) Pokrovsky, O. S.; Bronikowski, M. G.; Moore, R. C.; Choppin, G. R. *Radiochim. Acta* **1998**, 80, 23–29.
- (19) Bhat, T. R.; Krishnamurthy, M. J. *Inorg. Nucl. Chem.* **1964**, 26, 587–594.
- (20) Borkowski, M.; Lis, S.; Choppin, G. R. *Radiochim. Acta* **1996**, 74, 117–121.
- (21) Rajan, K. S.; Martell, A. E. *Inorg. Chem.* **1965**, 4, 462–469.
- (22) Tananaev, I. V.; Rodicheva, G. V. *Atomic Energy* **1963**, 14, 395/9, 401–404.
- (23) *Gmelin Handbook of Inorganic Chemistry*, Supplement Vol. C14; Springer-Verlag: New York, 1981; p 112.
- (24) Langmuir, D. *Geochim. Cosmochim. Acta* **1978**, 42, 547–569.

Received for review November 8, 1999. Revised manuscript received February 14, 2000. Accepted March 1, 2000.

ES991251E